Hindawi
Scientific Programming
Volume 2022, Article ID 3041911, 17 pages
https://doi.org/10.1155/2022/3041911

Research Article

Study on the Combination of Pump Rod Pipe in Complex Structure

Dongxu He

Zhuangxi Oil Production Plant, Shengli Oilfield Branch, SINOPEC, Dongying, Shandong 257237, China

Correspondence should be addressed to Dongxu He; 2018212615@mail.chzu.edu.cn

Received 24 June 2022; Revised 5 August 2022; Accepted 12 August 2022; Published 13 September 2022

Academic Editor: Punit Gupta

The 3-D mechanical model of the inclined shaft pumping pump and the optimization model of anti-partial wear structure and security position are established in this paper. Based on the real data of well, 148-inclined 2 slope measurement, the ordinary pipe rod combination, inclined well pumping pump lining oil pipe, and oil pump laser oil pipe are optimized and calculated. In order to improve the computing power and reduce computational time consumption, this paper uses cloud computing technology in the computing process. The results show that the combination method of the lining oil pipe and the ordinary continuous pumping rod has less axial force and lateral force, and finally, the combination method of different well pipes is obtained.

1. Introduction

The pumping unit has the characteristics of large quantity and wide range, which is the primary way of oil production at home and abroad. China's pumping unit technology has been relatively mature, but in recent years, the oil pumping machine well's mining environment has become more complex. Oil well sand, gas, thick oil reservoirs, and significant slopes are all critical problems faced by oil well mining. Especially for large slope Wells, the slender pumping rod column works in the eyes of the curved well, resulting in serious partial grinding of the rod pipe, low pump efficiency of the pumping pump, shortening of the pump inspection cycle, reduction of the efficiency of the oil well system and other problems. A variety of special oil pumping pumps have been developed at home and abroad to adapt to the harsh mining environment, reduce the adverse effects of these factors, improve the pump efficiency, and ensure the normal production of oil Wells. Therefore, it is proposed to carry out the optimization and research project of the lifting process of complex structure Wells. According to the characteristics of the commonly used inclined well pumping pump in complex structure Wells, the force model of inclined well pumping pump and the whole 3-D pumping rod and column mechanical model can analyze the influence of each factor on the efficiency of the oil well system. According to the structural characteristics of complex structure shaft structure, the establishment of anti-partial wear structure combination and security position optimization model, the development of reasonable anti-partial wear combination, and optimization of pumping parameters of pumping machine is of great significance to improve the pump efficiency of inclined well pumping pump under meeting the safety and life conditions.

Since the 1940s, the rod pump lifting system behavior predicts and simulates the data provided by the test and the computer simulation technology. The simulated results are compared with the field measured data and applied to the evaluation and optimization design and fault diagnosis of the rod extraction system. From the calculation methods and characteristics used in each period, they are mainly divided into three calculation methods: Approximation formula calculation method [1, 2], API computational method [3, 4], and Numerical simulation and calculation method [5].

At present, the basic idea of mechanical model establishment is as follows: The external forces and internal forces of infinitesimals is studied by taking the deformed rod and column infinitesimals as the object. Then, the mechanical model of infinitesimals is established according to Newton's second Law of motion and the equilibrium principle.

Earlier studies took a segment of the infinitesimal of the pumping rod column in the well eye, and assumed that the infinitesimal segment is an arc in the spatial oblique plane. The wellbore curvature of the rod and column infinitesimal is constant, and the shear force on the rod and column cross-section is ignored, and the spatial distribution of the oil pipe axis and the shaft trajectory axis is consistent, and the rod and column are in continuous contact with the oil pipe. Obviously, several conditions as the initial hypothesis will lead to a large deviation of the calculation results, and the subsequent relevant studies have made a lot of improvements in these aspects.

Taking the ordinary inclined well as the example, Feng et al. established the force balance equation of rod and column by considering the change of azimuth angle. A simplified mechanical model of friction resistance and axial load in the upper and lower stroke is derived and the important parameters of friction resistance, axial load and axial deformation are analyzed and calculated. According to the example calculation results, the calculation results of friction resistance and axial load can provide a reliable basis for drilling equipment selection, optimizing rod and column parameters and well body structure [6].

Liu et al. analyzed and calculated the movement state of the pumping rod and column, and the various friction forces of the oil well [7]. Moreover, the constraints of the pumping rod column and the changes of the well slope and azimuth angle are considered comprehensively, and the 3-D stress model of the pumping rod column is established.

A general model for calculating the axial load of the eye shaft and column in any well is established by Tian et al. based on the friction force between the underground rod and pipe under the three-dimensional well eye track. The additional force is generated by the bending, the friction resistance is caused by the fluid in the pipe and the vibration load [8]. This model can be used to analyze and check the production and operation poles in any borehole track well.

Zhang et al. analyzed the motion state of the pumping rod column in the horizontal well, considered the inconsistency between the plunger and the suspension point motion, and found the position and time of the maximum and minimum force [9].

Kun et al. analyzed the current problems of rod and tube partial grinding theory and analyzed the influence of well fluid flow on the force of pumping rod and column [10]. The calculation model of the well fluid flow in the annular space of pumping rod and pipe is presented by their research.

In conclusion, because several assumptions of the initial mechanical model will cause the force calculation of the pumping rod and column of the inclined shaft pumping pump, the researchers do a lot of correction work. The main points of correction include: azimuth, column stiffness, friction resistance, and the influence of well fluid flow.

At present, there are many types of rod pump lifting in the west pile area, with complex well condition, and problems such as rod pipe disconnection, oil pipe grinding, and low machine production efficiency still exist. Theoretical support of machine production optimization is urgently needed to improve the oil production system of pumping machine.

In view of this, the keys of this study are as follows:

(1) The three-dimensional mechanical model of the complex structure shaft is established and solved.

(2) The anti-partial wear structure combination and security position optimization model are established to complete the anti-partial wear structure optimization (Lining oil pipe + continuous rod, laser oil pipe + continuous rod, continuous rod + ordinary oil pipe pumping rod).

2. Models and Equations

2.1. Three-Dimensional Mechanical Model of Inclined Shaft Pumping Pump. Generally, directional well trajectory have well sections with large curvature changes of the well trajectory. Because the string is constrained by the 3-D curved hole, the pipe column stiffness and the curvature of the shaft will affect the mechanical behavior of the pipe column during the operation. Therefore, the influence of the pipe column stiffness and the wellhole curvature on the pipe column force needs to be fully considered in the curved well section. The paper will establish a 3-D mechanical model considering the pumping rod and column stiffness of the inclined shaft pumping pump to describe the force situation of the pipe column in the curved shaft section.

The natural coordinate system O_sTNB is taken on the axis of the pipe column, and the infinitesimal body with any arc length of ds on the column was taken as the object of force analysis and is shown in Figure 1. Point A and point B are taken as the initial point and the end point, and their curve coordinates are s and $s + ds$. The force analysis of the infinitesimal was carried out on the basis of comprehensively considering the influence of the load, concentrated force, and torque of each division.

2.1.1. Geometric Equation. According to the basic principles of differential geometry,

$$\begin{cases} \overrightarrow{e_t} = \dfrac{dx}{ds}\overrightarrow{x} + \dfrac{dy}{ds}\overrightarrow{y} + \dfrac{dz}{ds}\overrightarrow{z}, \\ \overrightarrow{e_n} == \dfrac{1}{K}\left(\dfrac{d^2x}{ds^2}\overrightarrow{x} + \dfrac{d^2y}{ds^2}\overrightarrow{y} + \dfrac{d^2z}{ds^2}\overrightarrow{z}\right), \\ \overrightarrow{e_b} = \overrightarrow{e_t} \times \overrightarrow{e_n} = b_x\overrightarrow{x} + b_y\overrightarrow{y} + b_z\overrightarrow{z}, \end{cases} \tag{1}$$

where

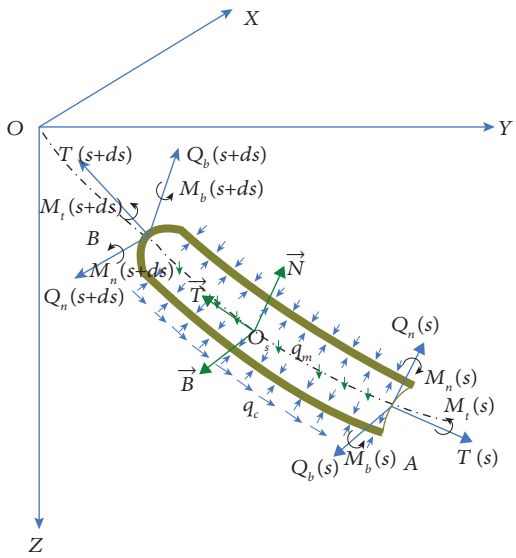

Figure 1: Schematic representation of the infinitesimal force analysis.

$$\begin{cases} \dfrac{dx}{ds} = -\sin\alpha\cos\phi, \\ \dfrac{dy}{ds} = -\sin\alpha\sin\phi, \\ \dfrac{dz}{ds} = -\cos\alpha, \end{cases} \tag{2}$$

$$\begin{cases} \dfrac{d^2x}{ds^2} = K_\alpha\cos\alpha\cos\phi - K_\phi\sin\alpha\sin\phi, \\ \dfrac{d^2y}{ds^2} = K_\alpha\cos\alpha\sin\phi + K_\phi\sin\alpha\cos\phi, \\ \dfrac{d^2z}{ds^2} = -K_\alpha\sin\alpha, \end{cases} \tag{3}$$

$$\begin{cases} b_x = \dfrac{-\left(K_\alpha\sin\phi - K_\phi\sin\alpha\cos\alpha\cos\phi\right)}{K}, \\ b_y = \dfrac{\left(K_\alpha\cos\phi - K_\phi\sin\alpha\cos\alpha\sin\phi\right)}{K}, \\ b_z = \dfrac{\left(K_\phi\sin^2\alpha\right)}{K}. \end{cases} \tag{4}$$

The unit vector in the gravity direction is $\vec{e_g}$, so $\vec{e_g} = \vec{z}$,

$$\begin{cases} \vec{e_g}\cdot\vec{e_t} = -\cos\alpha, \\ \vec{e_g}\cdot\vec{e_n} = -\dfrac{K_\alpha}{K}\sin\alpha, \\ \vec{e_g}\cdot\vec{e_b} = -\dfrac{K_\phi}{K}\sin^2\alpha, \end{cases} \tag{5}$$

$$\begin{cases} K = \left|\dfrac{d^2\vec{r}}{ds^2}\right| = \sqrt{K_\alpha^2 + K_\phi^2\sin^2\alpha}, \\ K_\alpha = \dfrac{d\alpha}{ds}, \\ K_\phi = \dfrac{d\phi}{ds}, \end{cases} \tag{6}$$

where α is the angle of deviation, rad.

ϕ is the well oblique orientation Angle, rad.

K_α is the well slope change rate, rad/m.

K_φ is the bearing rate, rad/m

K is the hole curvature, rad/m.

2.1.2. Equilibrium Equation. According to the condition characteristics of inclined shaft pump, the load of the pipe column in the well eye includes the dead weight of the pipe column, the support force of the pipe column and the well wall, the friction resistance, the internal and external fluid pressure, the viscous friction of the fluid, and the temperature load. Therefore, according to the stress condition, the infinitesimal section of the pipe column is analyzed as follows:

(a) Internal force and internal torque at both ends.

As shown in Figure 1, the concentration force $\vec{F}(s)$ at the curve coordinate S (point A) is

$$\vec{F}(s) = \left(Q_n(s)Q_b(s)\right)\begin{pmatrix} \vec{t}(s) \\ \vec{n}(s) \\ \vec{b}(s) \end{pmatrix}. \tag{7}$$

Centralized moment $\vec{M}(s)$ at the curve coordinate S (point A) is:

$$\vec{M}(s) = \left(M_\tau(s)M_n(s)M_b(s)\right)\begin{pmatrix} \vec{t}(s) \\ \vec{n}(s) \\ \vec{b}(s) \end{pmatrix}. \tag{8}$$

Centralized force $\vec{F}(s+ds)$ at the infinitesimal segment $s+ds$ (point B) is:

$$\vec{F}(s+ds) = \left((T+dT) - \left(Q_n + dQ_n\right) - \left(Q_b + dQ_b\right)\right) \cdot \begin{pmatrix} \vec{t}(s) + d\vec{t} \\ \vec{n}(s) + d\vec{n} \\ \vec{b}(s) + d\vec{s} \end{pmatrix}, \tag{9}$$

$$\vec{F}(s+ds) = \begin{pmatrix} -T(s) - dT(s) + k_0 Q_n(s)ds \\ -Q_n(s) - dQ_n(s) - \left[k_0 T(s) - \tau_0 Q_b(s)\right]ds \\ -Q_b(s) - dQ_b(s) - \tau_0 Q_n(s)ds \end{pmatrix}^T \cdot \begin{pmatrix} \vec{t}(s) \\ \vec{n}(s) \\ \vec{b}(s) \end{pmatrix}. \tag{10}$$

Centralized torque $\overrightarrow{M}(s+ds)$ at the infinitesimal segment $s+ds$ (point B) is:

$$\overrightarrow{M}(s+ds) = \begin{pmatrix} -\left(M_t(s) + dM_t(s)\right) \\ -\left(M_n(s) + dM_n(s)\right) \\ -\left(M_b(s) + dM_b(s)\right) \end{pmatrix}^T \cdot \begin{pmatrix} \vec{t}(s) + d\vec{t} \\ \vec{n}(s) + d\vec{n} \\ \vec{b}(s) + d\vec{s} \end{pmatrix}, \tag{11}$$

$$\overrightarrow{M}(s+ds) = \begin{pmatrix} -M_t(s) - dM_t(s) + k_0 M_n(s)ds \\ -M_n(s) - dM_n(s) - \left[k_0 M_t(s) - \tau_0 M_b(s)\right]ds \\ -M_b(s) - dM_b(s) - \tau_0 M_n(s)ds \end{pmatrix}^T \begin{pmatrix} \vec{t}(s) \\ \vec{n}(s) \\ \vec{b}(s) \end{pmatrix}. \tag{12}$$

(b) Dead weight of pipe column.

Dead weight is a part of the load of the pipe column on the overall force. In the straight well, the load is the weight of the pipe column itself, while in the curved well eye, it needs to be decomposed in all directions. Meanwhile, due to the formation fluid, the column will be subject to fluid buoyancy. Therefore, the floating weight is used for the analysis in the calculation. Column float weight per unit length q_m is

$$q_m = q \cdot K_f, \tag{13}$$

where K_f is the floating force coefficient; q is the unit weight of the tube string in the air, kN/m.

The dead weight load vector of the pipe column in the eye of the curved well can be expressed as:

$$\overrightarrow{f_G}(s) = \begin{pmatrix} q_m \cos\alpha & -q_m \dfrac{\sin\alpha}{k_0}\dfrac{d\alpha}{ds} & q_m \dfrac{\sin^2\alpha}{k_0}\dfrac{d\phi}{ds} \end{pmatrix} \begin{pmatrix} \vec{t}(s) \\ \vec{n}(s) \\ \vec{b}(s) \end{pmatrix}. \tag{14}$$

(c) Support anti-force.

Under the action of dead weight, the pipe column will be subjected to the support and reverse force of the well wall:

$$\vec{N} = N_n \vec{n} + N_b \vec{b}, \tag{15}$$

$$N^2 = N_n^2 + N_b^2. \tag{16}$$

(d) Friction between the well wall.

$$\vec{q}_c(s) = \left(\pm \mu_\alpha N \, \mu_t N_n \, \mu_t N_b\right) \begin{pmatrix} \vec{t}(s) \\ \vec{n}(s) \\ \vec{b}(s) \end{pmatrix}, \tag{17}$$

$$N^2 = N_n^2 + N_b^2, \tag{18}$$

where N_n is the positive pressure in the main normal direction, kN; N_b is the positive pressure in the subnormal direction, kN; μ_t is the friction coefficient in the circumferential directio; μ_α is the friction coefficient of the axis direction.

(e) Internal and external fluid forces.

During the water injection operation, there is high pressure injection liquid in the TUPIPE, external bore liquid pressure and injection pressure. Therefore, a set of axial "fictitious forces" are be generated on the pipe column during the operation. Under the action of internal pressure, the equivalent axial compression force at both ends of the microsegment can be expressed as:

$$\overrightarrow{P_i}(s) = P_i(s) A_i \vec{t}(s), \tag{19}$$

$$\overrightarrow{P_i}(s+ds) = \begin{pmatrix} A_i\left[P_i(s) + dP_i(s)\right] & k_0 A_i P_i(s)ds & 0 \end{pmatrix} \cdot \begin{pmatrix} \vec{t}(s) \\ \vec{n}(s) \\ \vec{b}(s) \end{pmatrix}, \tag{20}$$

where A_i is the cross-sectional area of oil lumen, m^2; P_i is the pressure in the tubing, MPa.

Similarly, under the external pressure, the two ends are subjected to a pair of equivalent axial tensile forces:

$$\begin{aligned}\overrightarrow{P_o}(s) &= -P_o(s)A_o\overrightarrow{t}(s)\\ \overrightarrow{P_o}(s+ds) &= -\left[\overrightarrow{P_o}(s)+d\overrightarrow{P_o}(s)\right]\\ &= \left(-A_o\left[P_o(s)+dP_o(s)\right]\ -k_0A_oP_o(s)ds\ \ 0\right)\\ &\quad\cdot\begin{pmatrix}\overrightarrow{t}(s)\\ \overrightarrow{n}(s)\\ \overrightarrow{b}(s)\end{pmatrix},\end{aligned} \tag{21}$$

where A_o is the cross-sectional area of oil lumen, m^2; P_o is the pressure in the tubing, MPa.

(f) Fluid viscosity and friction resistance.

The viscous friction resistance of the pipe wall subjected to the fluid can be expressed as:

$$\overrightarrow{f_\lambda} = -\nu\left[\frac{2\pi R\tau_f}{\sqrt{\nu^2+(R\omega)^2}}+\frac{2\pi R\mu}{\ln\left(D_w/2R\right)}\right]\vec{t}(s), \tag{22}$$

where τ_f is the fluid structure force, N/m; μ is the fluid dynamical viscosity, Ns/m^2; ω is the column rotation angular speed, rad/s; D_w is the well eye diameter, m; R is the outer radius of pipe column, m; ν is the fluid speed, m/s.

The force balance condition $\sum \underset{F}{\longrightarrow} = 0$:

$$\begin{aligned}&\vec{F}(s)\vec{F}(s+ds)+\vec{q}c\,ds+\overrightarrow{f_G}\,ds+f+\overrightarrow{P_i}(s)+\overrightarrow{P_i}(s+ds)\\ &\quad+\overrightarrow{P_o}(s)+\overrightarrow{P_o}(s+ds)+d\overrightarrow{F_i}(s)+d\overrightarrow{F_o}(s)=0.\end{aligned} \tag{23}$$

Put all expressions of stress into (2–24). Ignoring trace product, and the project of it to the tangent direction $\overrightarrow{t_0}$, main normal direction $\overrightarrow{n_0}$ and subnormal direction $\overrightarrow{b_0}$ is:

$$\begin{cases}\dfrac{dT_t(s)-dP_i(s)A_i+dP_o(s)A_o}{ds}-k_0Q_n(s)=q_m\cos\alpha-\mu_\alpha N-f_\lambda,\\[2ex] \dfrac{dT_n(s)}{ds}+K_0\left[Q_t(s)-P_i(s)A_i+P_o(s)A_o\right]+\tau_0Q_b(s)=N_n-\mu_tN_b-q_m\dfrac{\sin\alpha}{K_0}\dfrac{d\alpha}{ds},\\[2ex] \dfrac{dF_b(s)}{ds}+\tau_0Q_n(s)=-N_b-\mu_tN_n+q_m\dfrac{\sin^2\alpha}{K_0}\dfrac{d\phi}{ds}.\end{cases} \tag{24}$$

Then according to the torque equilibrium condition $\sum \overrightarrow{M} = 0$:

$$\begin{cases}\dfrac{dM_t}{ds}=\mu_tRN+2\pi R^3\omega\left[\dfrac{\tau_f}{\sqrt{\nu^2+(R\omega)^2}}+\dfrac{2\mu}{D_w-2R}\right],\\[2ex] \dfrac{dM_b}{ds}=Q_n,\\[2ex] \tau\cdot M_b+K\cdot M_t=Q_b.\end{cases} \tag{25}$$

2.1.3. Physical Equations. In the well-hole track, the transverse deformation of the pipe column is constrained by the wellhole, and the deformation is still within the elastic deformation range, so the physical relationship of the oil pipe deformation is:

$$\begin{aligned}M_b &= EIK,\\ \frac{dM_b}{ds} &= EI\frac{dK}{ds},\\ \frac{d^2M_b}{ds^2} &= EI\frac{d^2K}{ds^2},\end{aligned} \tag{26}$$

where E- is the Young's modulus of elasticity, kN/m^3; I is the moment of inertia of the tube column, m^4.

Organize the formula (1–25) to (26):

$$\begin{cases} \dfrac{dT_t - dP_iA_i + dP_oA_o}{ds} + K \cdot EI\dfrac{dK}{ds} \pm \mu_\alpha N + f_\lambda - q_m \cos\alpha = 0, \\ \dfrac{dM_t}{ds} = \mu_t RN + 2\pi R^3 \omega \left[\dfrac{\tau_f}{\sqrt{v^2 + (R\omega)^2}} + \dfrac{2\mu}{D_w - 2R} \right], \\ -EI\dfrac{d^2K}{ds^2} + K \cdot T + \tau\left(\tau \cdot EI\dfrac{dK}{ds} + KM_t \right) + N_n + \mu_t N_b + q_m \sin\alpha \dfrac{K_\alpha}{K} = 0, \\ -\dfrac{d\left(\tau \cdot EIK + KM_t\right)}{ds} - \tau \cdot EI\dfrac{dK}{ds} + \mu_t N_n - N_b - q_m \sin^2\alpha \dfrac{K_\varphi}{K} = 0, \\ N^2 = N_n^2 + N_b^2. \end{cases} \tag{27}$$

According to the close surface definition $\tau = 0$, the (30) is reduced to:

$$\begin{cases} \dfrac{dT_t - dP_iA_i + dP_oA_o}{ds} + K \cdot EI\dfrac{dK}{ds} \pm \mu_\alpha N + f_\lambda - q_m \cos\alpha = 0, \\ \dfrac{dM_t}{ds} = \mu_t RN + 2\pi R^3 \omega \left[\dfrac{\tau_f}{\sqrt{v^2 + (R\omega)^2}} + \dfrac{2\mu}{D_w - 2R} \right], \\ -EI\dfrac{d^2K}{ds^2} + K \cdot T + N_n + \mu_t N_b + q_m \sin\alpha \dfrac{K_\alpha}{K} = 0, \\ -K\dfrac{dM_t}{ds} + \mu_t N_n - N_b - q_m \sin^2\alpha \dfrac{K_\varphi}{K} = 0, \\ N^2 = N_n^2 + N_b^2. \end{cases} \tag{28}$$

The established model belongs to a system of nonlinear differential equations, which therefore can be solved by the quasi-Newton iteration method of the system of nonlinear equations. Choose the difference formula in the finite difference first:

$$\begin{cases} \dfrac{dT}{ds} = \dfrac{T(s+1) - T(s)}{h(s+1) - h(s)}, \\ \dfrac{dM_t}{ds} = \dfrac{M_t(s+1) - M_t(s)}{h(s+1) - h(s)}, \\ \dfrac{dK}{ds} = \dfrac{K(s+1) - K(s)}{h(s+1) - h(s)}, \\ \dfrac{d^2K}{ds^2} = \dfrac{K(s+2) - 2K(s+1) + K}{[h(s+1-h(s))]^2}, \end{cases} \tag{29}$$

where $h(s+1), h(s)$ is the segment length of each calculated segment, respectively.

The ordinary differential equations are discretized by using the above equation, we can get$T(s+1), M_t(s+1)$. The friction resistance F, friction torque M_t, and axial loading T at each calculation point of the column can be calculated by taking the above parameters into the nonlinear system of equations.

2.1.4. The Length of the Pumping Rod Anti-Centralizer Is Determined. As shown in Figure 2, due to the small radius of curvature of the wellhole, the pumping rod will make contact with the well wall, which will then accelerate the wear of the pumping rod when the pumping rod passes through two points: A and B in the wellhole track. In general, it is necessary to add two anti-grinding blocks to the extraction rod in order to prevent wear to reduce the life of the pumping rod. In this way, when the radius of curvature of the well is small, the anti-grinding block will contact with the well wall first to effectively protect the pumping rod.

In Figure 2, D is the diameter of the grinding block, d is the diameter of the pumping rod, R is the radius of curvature of the two points A and B in the well track, and L is the spacing between the two grinding blocks.

Where AC⊥CO, AO approximately equal to $R + 1/2D$, $CO = R + 1/2d$, the length of the AC can be obtained by the Pythagorean theorem:

$$AC = \sqrt{AO^2 - CO^2} = \sqrt{\left(R + \frac{1}{2}D\right)^2 + \left(R + \frac{1}{2}d\right)^2} = \sqrt{R(D-d) + \frac{1}{4}\left(D^2 - d^2\right)}. \tag{30}$$

The spacing L between the two grinding blocks can be approximately equal to two times AC:

$$L = 2 \times \sqrt{R(D-d) + \frac{1}{4}\left(D^2 - d^2\right)}. \tag{31}$$

3. Results and Discussion

3.1. Well Conditions Analysis of Pile 148-X2 Oil Well. According to the logging data of pile 148-X2 oil well given in Table 1, the well-hole track is fitted in 3-D, and the result curve is shown in Figure 3.

According to the data investigation of the machine mining well production conditions of the west pile oil production plant, the main machine mining parameters of the oil well and those of the inclined well pumping pump are given in Table 2.

3.2. Calculation Results of Common Pipe Combination of Pumping Pump in Pile 148-X2. According to the logging data of pile 148-X2 well given in Table 1 and the relevant data in the main parameters of Table 2, the axial force of pile 148-X2 oil well is calculated as shown in Figure 4.

According to Figure 4, the maximum axial force is at the wellhead, and the value is 62.7 kN.

The elongation of pile 148-X well is shown in Figure 5.

As is known by Figure 5, The maximum elongation is at a well depth of 1,988 m, the value is 0.9826 m.

The column curvature of pile 148-X2 well is shown in Figure 6.

According to Figure 6, the maximum curvature is at the well depth of 355.1 m, the value is 0.02735 m^{-1}. According to the well curvature data, the grinding block can be reasonably arranged at the large curvature position.

The lateral force of pile 148-X2 oil well is shown in Figure 7.

As is known by Figure 7, the maximum lateral force is at the depth of 269 meters in the well, the value is 137.7 N.

The safety factor of the whole well column of pile 148-X2 well is shown in Figure 8.

According to Figure 8, the minimum safety factor of the pumping rod is at the wellhead. The minimum safety value is 4.851, which is greater than the production process requirements, and the strength of the pumping rod in the whole well section meets the standard.

The installation spacing of anti-wear block in the whole well section of pile 148-X2 oil well is shown in Figure 9.

According to Figure 9, the installation spacing of anti-grinding block can be reasonably arranged to improve the wear of the pumping rod and improve the life of the pumping rod.

3.3. Optimization Culation Result of Lining of Inclined Pump of Pile 148-X2. According to Figure 7, in the 170 m-400 m and 810 m-930 m wells, the lateral force of the inclined well pumping pump stem is too large, which increases the safety risk. Therefore, the 170 m-400 m and 810 m-930 m well

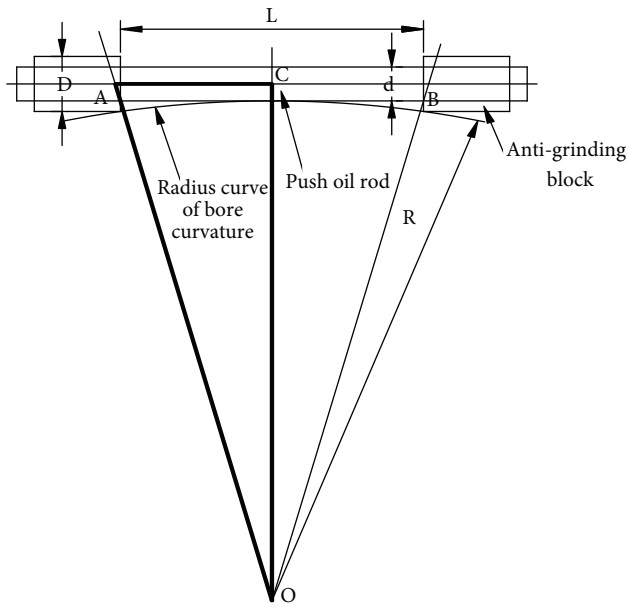

Figure 2: Geometric relationship of anti-grinding centralizer.

Table 1: 148-inclined 2 well oblique survey data.

	Well depth (m)	Angle of deviation (°)	Azimuth (°)
1	108.49	0.22	155.78
2	127.15	1.14	73.28
3	155.15	3.03	49.18
4	183.13	5.45	44.98
5	211.97	8.61	43.68
6	240.69	12.74	42.68
7	269.01	17.01	41.28
8	297.72	20.57	38.98
9	326.38	24.05	41.88
10	355.06	28.54	41.48
11	383.73	31.33	37.78
12	412.36	30.98	38.08
13	440.83	30.28	38.88
14	469.66	30.06	39.98
15	498.13	32.48	36.28
16	526.64	31.42	36.58
17	555.30	31.99	36.63
18	583.75	32.56	36.68
19	612.54	33.27	37.18
20	641.23	33.27	37.28
21	669.95	33.49	37.48
22	687.24	33.66	39.18
23	701.00	33.66	38.18
24	726.69	33.53	36.38
25	755.51	33.53	36.08
26	784.10	34.06	36.18
27	812.63	33.84	35.58
28	841.45	37.31	37.08
29	869.81	41.00	39.18
30	898.44	45.26	38.58
31	926.97	47.50	39.58
32	955.48	47.77	39.38
33	984.13	47.81	39.08
34	1012.88	47.24	39.08

Table 1: Continued.

	Well depth (m)	Angle of deviation (°)	Azimuth (°)
35	1041.46	48.56	39.28
36	1070.12	48.47	39.08
37	1098.96	48.16	38.98
38	1127.58	50.54	38.48
39	1156.15	52.34	37.88
40	1183.08	52.21	37.68
41	1211.92	51.81	37.48
42	1240.54	50.84	37.38
43	1269.11	52.43	36.28
44	1297.63	53.53	37.08
45	1326.39	53.22	37.08
46	1355.25	53.22	36.98
47	1383.98	52.51	37.08
48	1412.61	53.79	37.38
49	1441.49	54.14	37.08
50	669.95	33.49	37.48
51	1470.05	54.40	36.58
52	1498.75	55.77	36.38
53	1527.42	56.69	36.28
54	1585.07	54.49	37.18
55	1613.91	53.79	36.98
56	1642.64	53.17	37.08
57	1671.48	52.69	37.08
58	1700.16	51.81	37.08
59	1728.94	52.60	37.88
60	1757.64	53.75	38.28
61	1786.07	54.89	38.18
62	1814.85	54.62	38.08
63	1843.19	54.54	37.68
64	1873.02	54.58	37.98
65	1902.55	54.58	37.78
66	1931.10	56.07	37.08
67	1959.64	57.35	36.28
68	1988.32	56.82	35.58
69	2017.16	56.43	35.48
70	2045.74	55.81	37.28
71	2074.50	55.15	37.58
72	2103.10	53.79	37.18
73	2131.86	54.14	36.88
74	2160.27	54.84	37.58
75	2188.97	53.96	37.48
76	2217.75	54.27	37.38
77	2246.32	53.96	38.48
78	2275.12	54.10	39.08
79	2303.58	53.53	38.98
80	2332.21	52.91	38.88
81	2360.80	53.22	39.98
82	2389.42	54.71	39.68
83	2417.99	55.68	39.68
84	2446.74	55.77	39.98
85	2475.43	54.98	40.48
85	2504.20	54.18	39.48
87	2533.40	53.44	39.38
88	2561.62	52.73	39.28
89	2590.35	52.87	38.98
90	2619.10	53.70	40.08
91	2647.83	54.00	41.68
92	2676.54	54.01	40.98
93	2705.27	55.90	40.58
94	2733.86	57.57	39.28

Table 1: Continued.

	Well depth (m)	Angle of deviation (°)	Azimuth (°)
95	2762.52	57.83	37.38
96	2791.19	57.44	36.98
97	2819.88	58.40	37.08
98	2848.65	58.80	36.28
99	2877.29	59.19	35.88
100	2905.97	58.71	35.68

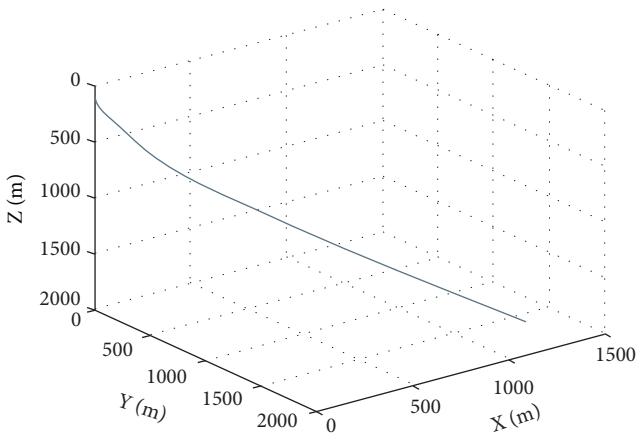

Figure 3: 3-D fitting curve of well-hole track of pile 148-X2 oil well.

Table 2: Main parameter.

	Parameter name	Value
1	Grading of oil pumping rod	3
2	Grade 1 pumping rod diameter (mm)	25
3	Grade 2 pumping rod diameter (mm)	22
4	Grade 3 pumping rod diameter (mm)	19
5	Grade 4 oil extraction rod diameter (mm)	10
6	Level 1 grade length (m)	549.8
7	Level 2 grade length (m)	572.81
8	Level 3 grade length (m)	863.24
9	Pump self-respect (kg)	50
10	Pump diameter (mm)	44
11	Pump gap (mm)	0.1
12	Number of swimming valves	2
13	Level 4 grade length (m)	450
14	Density of oil pumping rod (g/cm3)	7.85
15	Crude oil density (kg/m^3)	0.878
16	Axial friction coefficient	0.1
17	Oil pipe inner diameter (mm)	50.8
18	Wellhead back pressure (Pa)	0.6
19	Allow the stress of the suction rod (MPa)	867
20	Swimming valve plunger area (mm^2)	50
21	Valve hole cross-section (mm^2)	50
22	Crude oil sports viscosity (mm^2/s)	20
23	Valve hole flow coefficient	0.8

sections are selected with lined oil pipes to replace the ordinary oil pipes for pipe string combination optimization. The method can reduce the lateral force by reducing the friction force.

According to the logging data of pile 148-X2 well given in Table 1 and the relevant data in the main parameters of Table 2, the axial force of pile 148-X2 oil well is calculated as shown in Figure 10.

According to Figure 10, the maximum axial force is at the wellhead, the value is 43.23 kN.

The extension of pile 148-X2 is shown in Figure 11.

According to Figure 11, the maximum elongation value is at the well depth of 1,931 meters, and the value is 0.7034 m.

The column curvature of pile 148-X2 well is shown in Figure 12.

According to Figure 12, the maximum curvature is at the well depth of 326.4 m, and the value is 0.002735 m^{-1}. According to the well curvature data, the grinding block can be reasonably arranged at the large curvature position.

The lateral force of pile 148-X2 oil well is shown in Figure 13.

According to Figure 13, the maximum lateral force is at 240.7 meters of the well depth, and the value is 95.97 N.

The safety factor of the whole well column of pile 148-X2 well is shown in Figure 14.

According to Figure 14, the minimum safety factor of the pumping rod is at the wellhead, and the value is 7.037. The safety factor is greater than the production process requirements, and the strength of the pumping rod in the whole well section meets the standard.

The installation spacing of anti-wear block in the whole well section of pile 148-X2 oil well is shown in Figure 15.

According to Figure 15, the installation spacing of anti-grinding block can be reasonably arranged to improve the wear of the pumping rod and to improve the life of the pumping rod.

3.4. Optimized Calculation Results of Laser Oil Pipe of Inclined Pumping Pump of Pile 148-X2 Oil Well. According to the logging data of pile 148-X2 well given in Table 1 and the relevant data in the main parameters of Table 2, the axial force of pile 148-X2 oil well is calculated as shown in Figure 16.

According to Figure 16, the maximum axial force is at the wellhead, and the value is 50.4 kN.

The extension of pile 148-X well is Figure 17.

According to Figure 17, the maximum extension value is at the well depth of 1,931 m, and the value is 0.7981 m.

The column curvature of pile 148-X2 well is shown in Figure 18.

From Figure 18, the maximum curvature is at 355.1 m of the well depth, and the value is 0.002735 m^{-1}. According to the well curvature data, the grinding block can be reasonably arranged at the large curvature position.

The lateral force of pile 148-X2 oil well is shown in Figure 19.

According to Figure 19, the maximum lateral force is at the well depth of 240.7 meters, and the value is 110.6 N.

The safety factor of the whole well column of pile 148-X2 well is shown in Figure 20.

According to Figure 20, the minimum safety factor of the pumping rod is at the wellhead, and the minimum safety value is 6.035, The safety factor is greater than the production process requirements, and the strength of the pumping rod in the whole well section meets the standard.

The installation spacing of anti-wear block in the whole well section of pile 148-X2 oil well is shown in Figure 21.

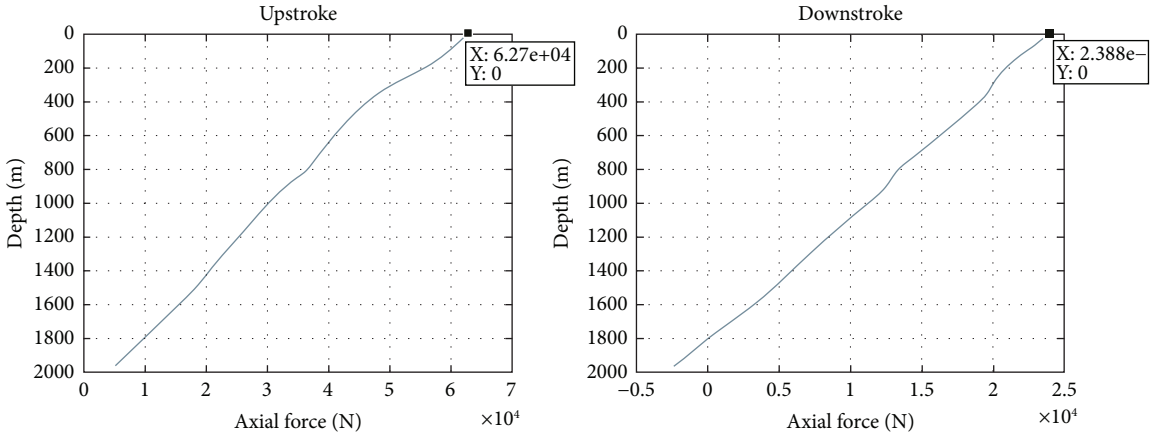

Figure 4: Pile 148-X2 well axial force.

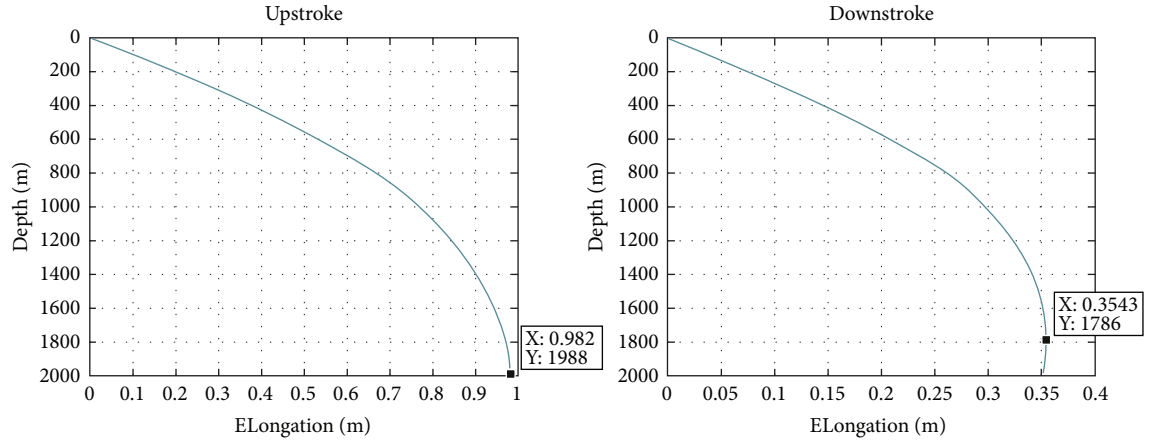

Figure 5: Lengation of well pile 148-X2.

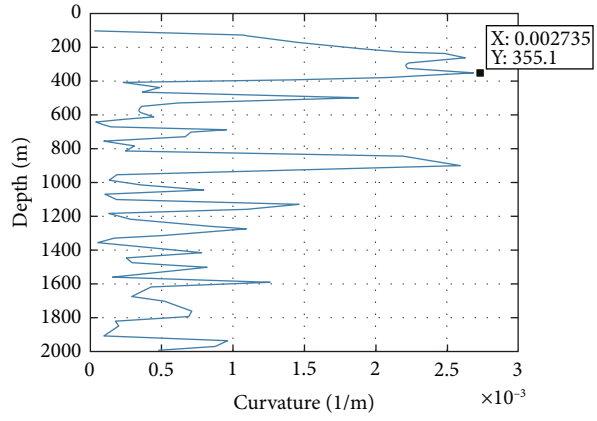

Figure 6: Pipe column curvature of well pile 148-X2.

According to Figure 21, the installation spacing of anti-grinding block can be reasonably arranged to improve the wear of the pumping rod and to improve the life of the pumping rod.

3.5. Analysis of the Preferred Results of the Inclined Well Pumping Pump. According to Figure 22, the inclined shaft pumping pump has minimum friction resistance under the combination of lining pipe and continuous

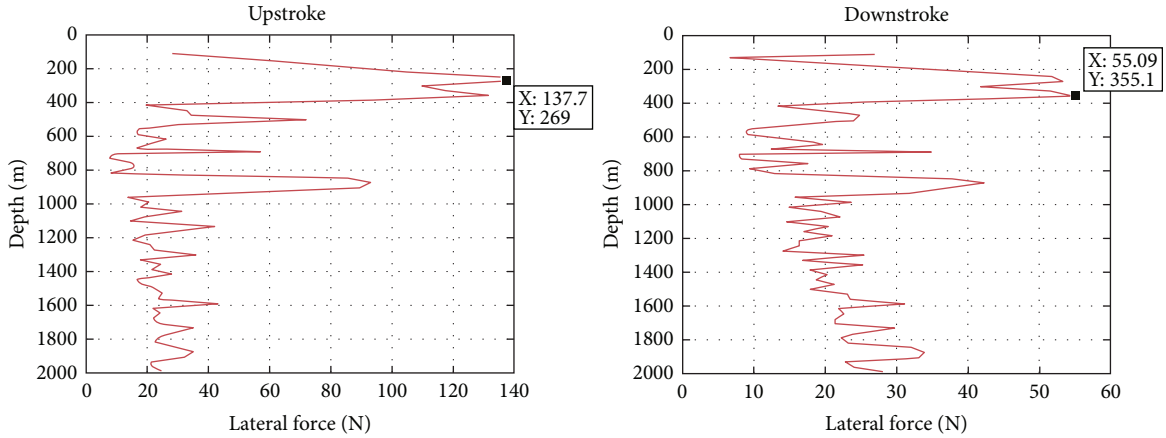

Figure 7: Column lateral force data of well pile 148-X2.

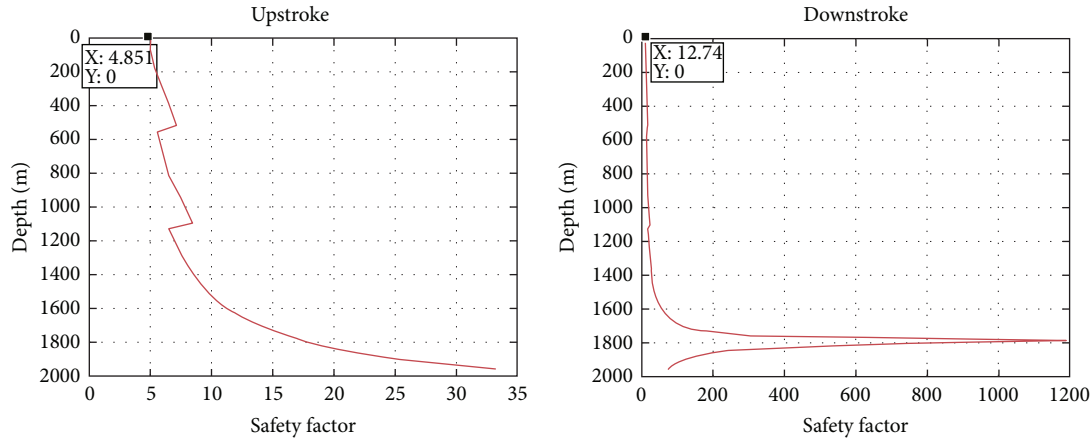

Figure 8: Safety factor of the pumping rod.

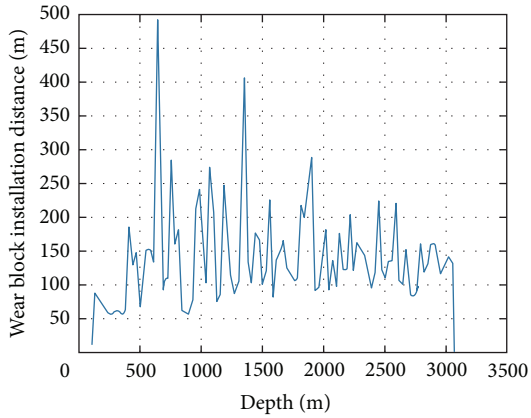

Figure 9: Installation spacing of anti-wear block in the whole well section of pile 136-X15.

suction rod. Compared with the ordinary inclined shaft pumping pump rod and pipe combination mode, the combination mode of lined oil pipe and continuous pumping rod can reduce the friction force by more than 30%, so as to achieve the effect of improving the pump effect.

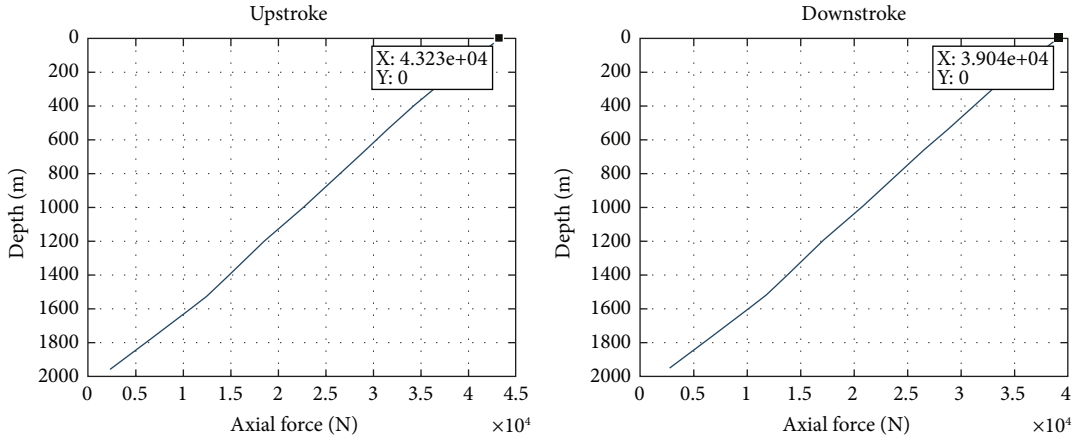

Figure 10: Axial force of pile 148-X2 well.

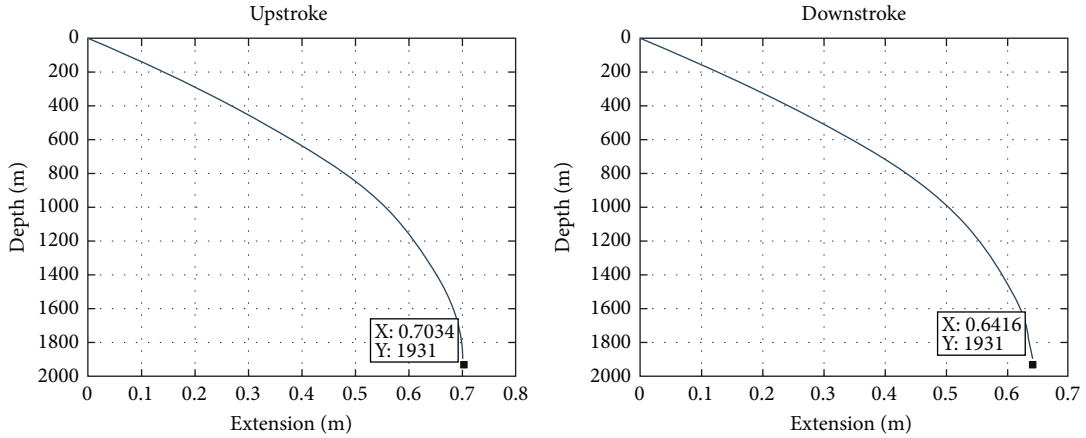

Figure 11: Extension of well pile 148-X2.

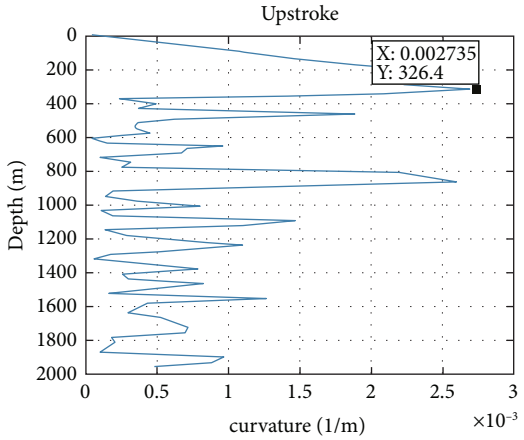

Figure 12: Pipe column curvature of well pile 148-X2.

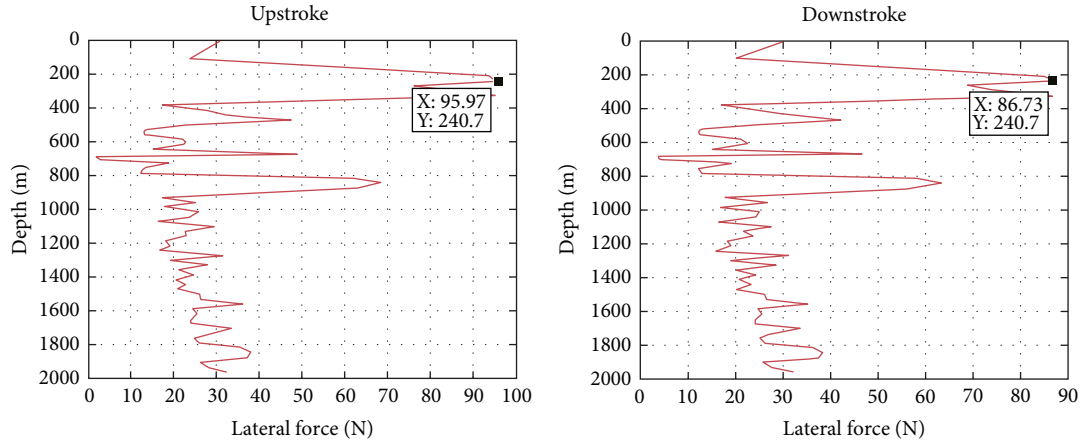

Figure 13: Column lateral force data of well pile 148-X2.

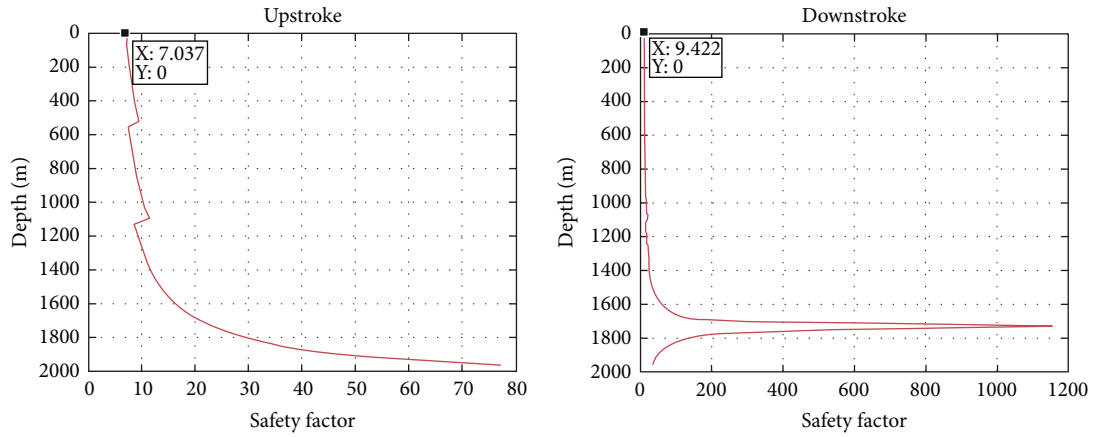

Figure 14: Safety factor of the pumping rod.

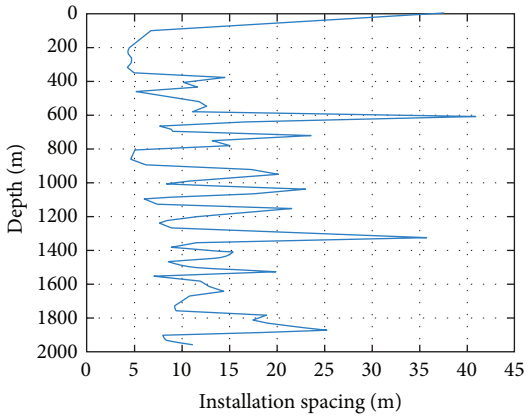

Figure 15: Installation spacing of anti-wear block in the whole well section of pile 136-X15.

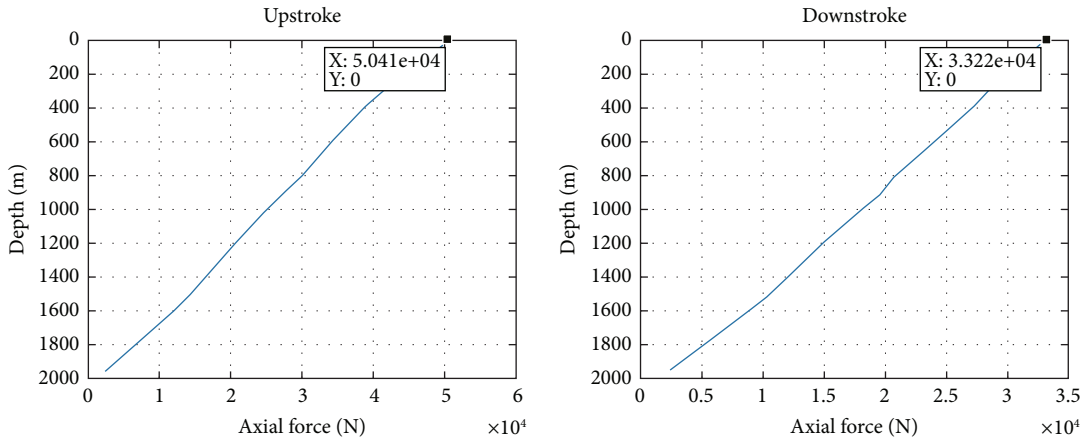

Figure 16: Axial force of pile 148-X2.

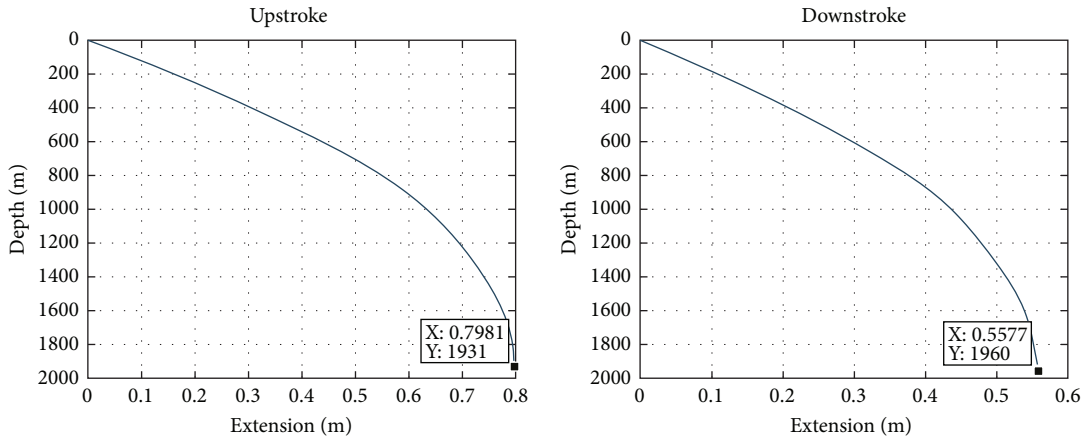

Figure 17: Extension of well pile 148-X2.

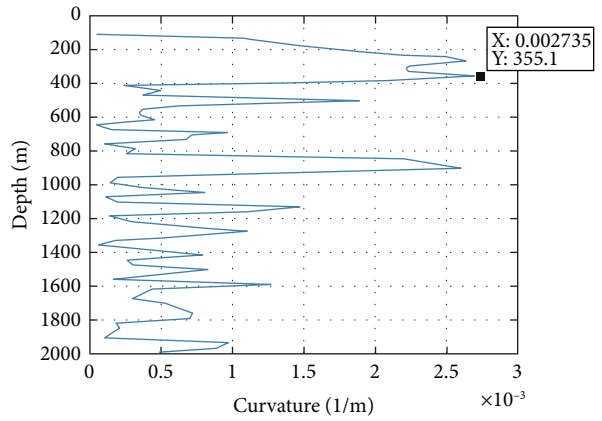

Figure 18: Pipe column curvature of well pile 148-X2.

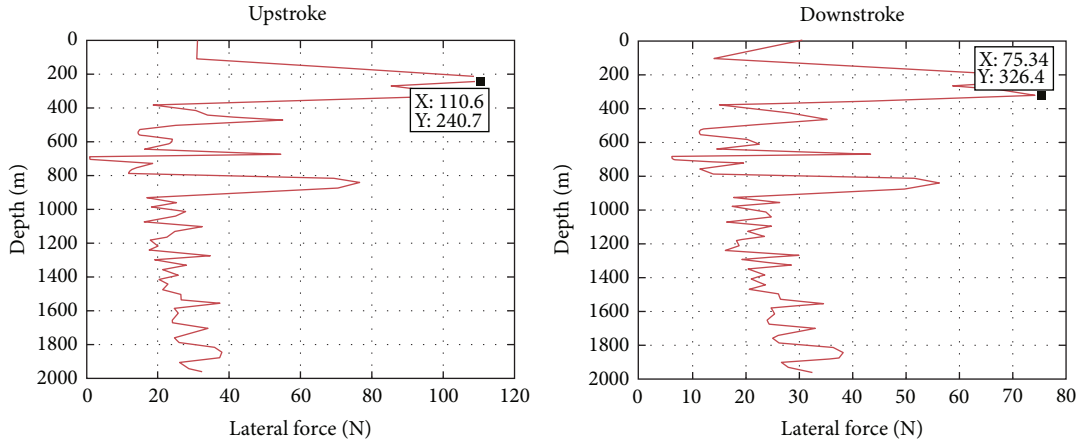

Figure 19: Lateral force of pile 148-X2 well pipe post.

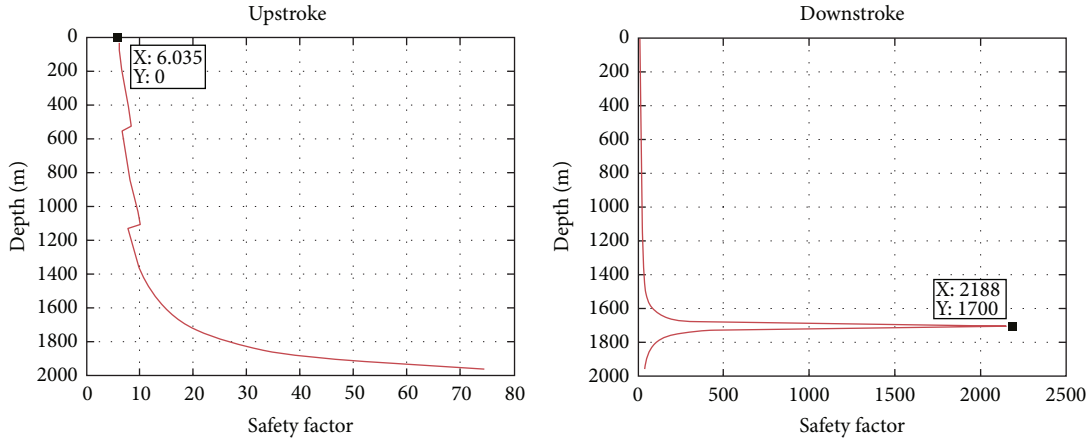

Figure 20: Safety factor of the pumping rod.

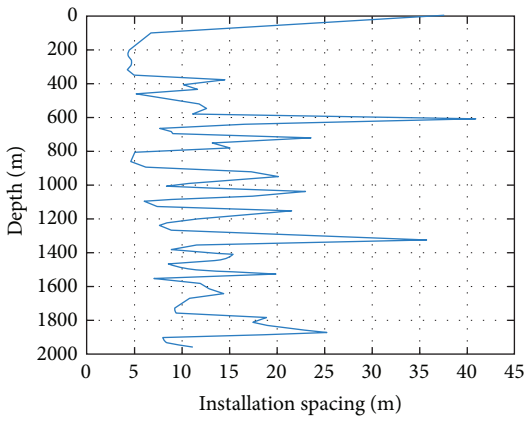

Figure 21: Installation spacing of anti-wear block in the whole well section of pile 136-X15.

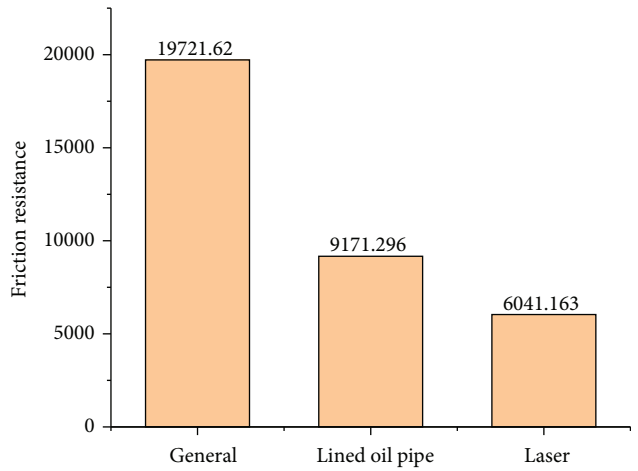

Figure 22: Comparison of rod and pipe optimization combination effect.

Table 3: Comparison of parameters of three different combinations of pipe combination.

	General pipe rod combination	Lined oil pipe rod and pipe combination	Laser tubing rod and pipe combination
Axial force (kN)	62.7	43.23	50.4
Extension (m)	0.9826	0.7034	0.7981
Lateral force (N)	137.7	95.97	110.6
Safety factor	4.851	7.037	6.035

Table 4: Pipe combinations of different well pipes.

Well section (m)	Combination mode of rod pipe
0–170	Combination of ordinary pumping pipe and continuous pumping rod
170–400	Lined pumping pipe and continuous pumping rod
400–440	Combination of ordinary pumping pipe and continuous pumping rod
440–500	Combination of laser pumping pipe and continuous pumping rod
500–780	Combination of ordinary pumping pipe and continuous pumping rod
780–900	Lined pumping pipe and continuous pumping rod
900–2000	Combination of ordinary pumping pipe and continuous pumping rod

In conclusion, the comparison of mechanical properties parameters of three different TUtubes is presented in Tables 3 and 4.

4. Conclusion

The combination of the lining oil pipe and the ordinary continuous pumping rod has smaller axial forces and lateral forces are compared with the other two combinations. For different well pipes, different rod and pipe combinations should be adopted.

Take the pile 148-X2 well for example, in well section 0–170, use the combination of ordinary pumping pipe and continuous pumping rod. In well section 170–400, use the lined pumping pipe and continuous pumping rod. In well section 400–440, use the combination of ordinary pumping pipe and continuous pumping rod. In well section 440–500, use the combination of laser pumping pipe and continuous pumping rod. In well section 500–780, use the combination of ordinary pumping pipe and continuous pumping rod. In well section 780–900, use the lined pumping pipe and continuous pumping rod. In well section 900–2000, use the combination of ordinary pumping pipe and continuous pumping rod.

The above combination method reduces the friction force between the pumping rod column and the pumping pipe of the inclined shaft pump by reducing the lateral force, thus improving the pump efficiency.

Data Availability

The datasets used and/or analyzed during the current study are available from the corresponding author on reasonable request.

Conflicts of Interest

The authors declare that they have no conflicts of interest.

References

[1] W. Zhou, "Study on lifting parameters of rod pump," *Journal of Petrochemical Industry University*, vol. 31, no. 6, pp. 28–32, 2018.

[2] Y. Yan, Z. Li, and C. Dong, "Analysis and tool design of rod pump lift anchor technology," *Petroleum Mine Machinery*, vol. 50, no. 2, pp. 54–59, 2021.

[3] T. Liu, "Study on calculation of derrick under API," *China Safety Production Science and Technology*, vol. 15, no. 12, pp. 66–71, 2019.

[4] N. P. Subodh, K. S. Dinesh, P. A. Durga, A. Manashi, and K. Anup, "Investigation of catastrophic failure of API grade pipes used for hydraulic oil in an Integrated Steel Plant," *Engineering Failure Analysis*, vol. 138, Article ID 106336, 2022.

[5] J. Xue, C. Chen, and Z. Yang, "Establishment and Application of 3 D mechanical model of pumping rod," *Petrochemical applications*, vol. 40, no. 11, pp. 75–79, 2021.

[6] F. Ding, J. Wang, and L. Qian, "Real axial force calculation and application of downhole pipe column," *Journal of Oil and Natural Gas*, vol. 38, no. 3, pp. 67–78, 2016.

[7] J. Liu, H. Zhao, and L. Xian, "Experimental study on the mechanical responses of downhole tools in highly-deviated waterflooding well," *Journal of Petroleum Science and Engineering*, vol. 171, pp. 495–506, 2018.

[8] J. Tian, T. Zhou, and Yu Yao, "Analysis model of directional well wellhole trajectory under the action of drill column vibration," *Mechanical Design and Manufacturing*, no. 3, pp. 25–28, 2019.

[9] J. Zhang and H. Yan, "Deflection of eccentric tubes under axial loading in curved wellbores," *Journal of Petroleum Science and Engineering*, vol. 208, Article ID 109527, 2022.

[10] L. Kun, W. Xian, and H. B. Gao, "Fault diagnosis for downhole conditions of sucker rod pumping systems based on the FBH-SC method," *Petroleum Science*, vol. 12, no. 01, pp. 135–147, 2015.